P-4-2 (Invited)

Extended Abstracts of the 2014 International Conference on Solid State Devices and Materials, Tsukuba, 2014, pp1048-1049

METAL-CNT CONTACTS

Patrick Wilhite, Anshul A. Vyas, and Cary Y. Yang

Center for Nanostructures, Santa Clara University, Santa Clara, CA, U.S.A.
E-mail: cyang@scu.edu

Abstract

To realize carbon nanotube (CNT) as on-chip interconnect materials, the metal-CNT contact resistance must be well understood and minimized. In this study, we compile existing published results and understanding for two metal-CNT contact geometries, sidewall or side contact and end contact, and address their key performance characteristics. Analyses of high-resolution images of interface nanostructures for various metal-CNT structures, along with their measured electrical characteristics, provide the necessary knowledge for continuous improvements of techniques to reduce contact resistance.

1. Introduction

Carbon-based nanostructures (or nanocarbons) such as carbon nanotubes (CNTs) [1–6], carbon nanofibers (CNFs) [7–9], and graphene [10–13] are candidate materials for next-generation semiconductor devices and integrated circuits (IC) due to their tolerance to electromigration under high currents and excellent electrical, thermal, and mechanical properties [14 – 24]. Nanocarbons show increasing promise to replace copper (Cu) for on-chip interconnects and through-silicon-vias in three-dimensional chips [25, 26], largely because of their excellent controllability for directional growth and high current capacity. The key performance-limiting factor for nanocarbons remains the high contact resistance originating from the interface with metal electrodes [27], due to work function difference between the two materials [28,29]. It can also result from defects at and/or near the interface [28, 30] which introduce physical and chemical changes in either or both contacting materials. In the following sections, research on side-contacted and end-contacted metal-CNT interfaces is reviewed.

2. Side-Contacted Structures

One widely used methods for fabricating side-contacted metal-CNT structures consists of suspending a purified mixture of CNTs in an alcohol solution, which is then sonicated to de-bundle the CNTs, and then drop-casted on pre-patterned electrodes. Typical as-fabricated resistance values range from 10^4 to 10^9 Ω. Our experiments show that the initial *I-V* behavior tends to be highly nonlinear and asymmetric, and these initial resistances drop to the kΩ range after stressing with a current of 10^5 ~ 10^6 A/cm^2. Since no appreciable degradations are observed in the CNT nanostructure using high-resolution electron microscopy, this drastic reduction in the total resistance is attributed to decrease in the contact resistance induced by localized Joule heating at the interface [14,31].

Apart from current stressing, a widely used contact engineering approach utilizes metal deposition by Electron Beam-Induced Deposition (EBID) or Ion Beam-Induced Deposition (IBID). Such techniques can be applied to improve the metal-CNT interface of an existing device. Comparisons of CNF device resistance reductions due to current stressing and IBID-tungsten (W) deposition are shown in Figure 1 [19]. The benefits of depositing W on the contacts are evident, which show low resistance that remains invariant under current stressing, suggesting that the contact resistance is minimized for these devices. Numerous metals can be deposited with IBID or EBID as long as a suitable source gas is available [32].

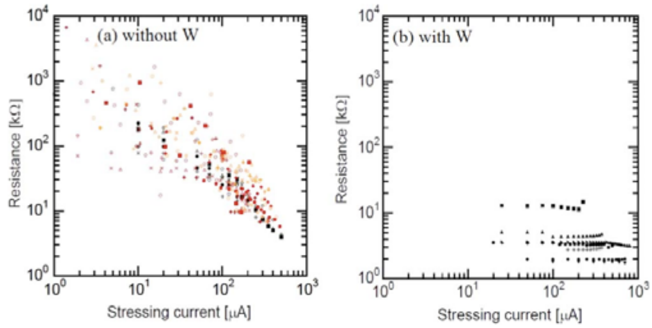

Fig. 1 Resistance of two-terminal CNF test devices vs. stress current for (a) without W and (b) with IBID-W deposited on CNF/Au electrode contacts [19].

3. End-Contacted Structures

For vertically aligned CNTs, it is natural to make end contacts at the as-grown interface with the metal underlayer, yielding lower contact resistance than that for side-contacted CNTs. Figure 2 shows a series of cross-sectional TEM images of metal-CNT (CNF in this case) interfaces grown on a Ti underlayer using plasma-enhanced chemical vapor deposition (PECVD). The interface regions display little evidence of impurities, and clearly show the graphitic planes nearly normal to the metal surface. From these images, it appears that the graphitic planes make direct contact to the Ti surface atoms, providing the necessary bonding to facilitate carrier transport and resulting in low contact resistance. In general, end-contacted geometries are advantageous over side contacts because of the absence of an interfacial layer or gap across which carrier tunneling occurs.

4. Conclusion

Contact resistance can be drastically reduced by Joule heating (current stressing, RTA, or electron beam irradiation) and through contact metallization using selection criteria governed by the wettability between the metal and CNT and work function difference. End-contacted vertical structures typically result in lower contact resistance due in large part to strong bonding between edge carbon and surface metal atoms. In a vertical configuration with a clean as-grown interface, the electrical conduction bottleneck is likely to be the as-deposited electrode or electrical probe. With further progress made in CNT growth and contact engineering, it is entirely conceivable that the end-contacted CNT structure will soon yield a total via resistance comparable to that of Cu in the most advanced IC technology node.

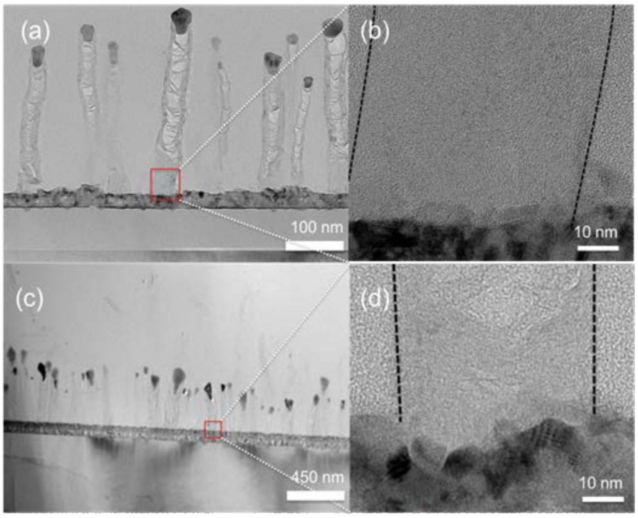

Fig. 2 (a) TEM cross-sectional image of as-grown CNTs on (a) smooth Ti substrate, and (b) HRTEM image of an individual CNT-metal interface as indicated in (a). (c) & (d) Corresponding images for a grainy Ti substrate. Both sets of interface images display a clean interface between CNT and underlayer metal [33].

References

[1] M. S. Dresselhaus, G. Dresselhaus, P. Avouris, *Carbon Nanotubes: Synthesis, Structure, Properties, and Applications*. Berlin/New York, Springer, 2001.

[2] S. Ijima, *Nature,* **354**, 56-58, 1991.

[3] C. Dekker, *Physics Today,* **52**, 22-28, 1999.

[4] F. Kreupl, A. P. Graham, G. S. Duesberg, W. Steinhögl, M. Liebau, E. Unger, W. Hönlein, *Microelectron. Eng.,* **64**, 399-408, 2002.

[5] J. Li, Q. Ye, A. Cassell, H. T. Ng, R. Stevens, J. Han, M. Meyyappan, *Appl. Phys. Lett.,* **82**, 2491-2493, 2003.

[6] M. Nihei, A. Kawabata, D. Kondo, M. Horibe, S. Sato, Y. Awano, *Jpn. J. Appl. Phys.,* **44**, 1626, 2005.

[7] L. Zhang, D. Austin, V. I. Merkulov, A. V. Meleshko, K. L. Klein, M. A. Guillorn, D. H. Lowndes, M. L. Simpson, *Appl. Phys. Lett.,* **84**, 3972-3974, 2004.

[8] A. V. Melechko, V. I. Merkulov, T. E. McKnight, M. A. Guillorn, K. L. Klein, D. H. Lowndes, M. L. Simpson, *J. Appl. Phys.,* **97**, 041301, 39pp, 2005.

[9] Q. Ngo, T. Yamada, M. Suzuki, Y. Ominami, A. M. Cassell, L. Jun, M. Meyyappan, C. Y. Yang, *IEEE Trans. Nanotechnol.,* **6**, 688-695, 2007.

[10] A. K. Geim, K. S. Novoselov, *Nature Mater.,* **6**, 183-191, 2007.

[11] J. S. Moon, D. Curtis, M. Hu, D. Wong, C. McGuire, P. M. Campbell, G. Jernigan, J. L. Tedesco, B. VanMil, R. Myers-Ward, C. Eddy Jr., D. K. Gaskill, *IEEE Electron Device Lett.,* **30**, 650-652, 2009.

[12] S. Bae, H. Kim, Y. Lee, X. Xu, J. S. Park, Y. Zheng, J. Balakrishnan, T. Lei, H. R. Kim, Y. I. Song, Y. J. Kim, K. W. Kim, B. Özyilmaz, J. H. Ahn, B. H. Hong, S. Iijima, *Nature Nanotechnol.,* **5**, 574-578, 2010.

[13] J. S. Moon, D. Curtis, S. Bui, T. Marshall, D. Wheeler, I. Valles, S. Kim, E. Wang, X. Weng, M. Fanton, *IEEE Electron Device Lett.,* **31**, 1193-1195, 2010.

[14] A. Naeemi, J. D. Meindl, *Annu. Rev. Mater. Res.,* **39**, 255-275, 2009.

[15] E. Pop, D. Mann, J. Cao, Q. Wang, K. Goodson, H. Dai, *Phys. Rev. Lett.,* **95**, 155505, 2005.

[16] H. Li, C. Xu, K. Banerjee, *IEEE Des. Test. Comput.,* **27,** 20-31, 2010.

[17] M. F. L De Volder, S. H. Tawfick, R. H. Baughman, A. J. Hart, *Science,* **339**, 535-539, 2013.

[18] H. Kitsuki, T. Yamada, D. Fabris, J. R. Jameson, P. Wilhite, M. Suzuki, C. Y. Yang, *Appl. Phys. Lett.,* **92**, 173110, 3pp, 2008.

[19] T. Saito, T. Yamada, D. Fabris, H. Kitsuki, P. Wilhite, M. Suzuki, C. Y. Yang, *Appl. Phys. Lett.,* **93**, 102108-102108, 2008.

[20] T. Yamada, T. Saito, D. Fabris, C. Y. Yang, *IEEE Electron Device Lett.,* **30**, 469-471, 2009.

[21] M. Suzuki, T. Yamada, C. Y. Yang, *Appl. Phys. Lett.,* **90**, 083111, 3pp, 2007.

[22] T. Yamada, F. R. Madriz, C. Y. Yang, *IEEE Trans. Electron Devices,* **56**, 1834-1839, 2009.

[23] T. Yamada, H. Yabutani, T. Saito, C. Y. Yang, *Nanotechnology,* **21**, 265707, 5pp, 2010.

[24] 2011 International Technology Roadmap for Semiconductors, with 2012 updates, http://www.itrs.net/Links/2012ITRS/Home2012.htm.

[25] T. Wang, K. Jeppson, N. Olofsson, E. E. Campbell, J. Liu, *Nanotechnology, **20***, 485203, 6pp, 2009.

[26] J. U. Knickerbocker, C. S. Patel, P. S. Andry, C. K. Tsang, L. P. Buchwalter, E. J. Sprogis, H. Gan, R. R. Horton, R. J. Polastre, S. L. Wright, J. M. Cotte, *IEEE J. of Solid-State Circuits,* **41**, 1718-1725, 2006.

[27] F. Wakaya, K. Katayama, K. Gamo, *Microelectron. Eng.,* **67**, 853-857, 2003.

[28] S. C. Lim, J. H. Jang, D. J. Bae, G. H. Han, S. Lee, I. S. Yeo, Y. H. Lee, *Appl. Phys. Lett.,* **95**, 264103, 3pp, 2009.

[29] T. Yamada, T. Saito, M. Suzuki, P. Wilhite, X. Sun, N. Akhavantafti, D. Fabris, C. Y. Yang, *J. Appl, Phys.* **107**, 044304, 5pp, 2010.

[30] C. Lan, D. N. Zakharov, R. G. Reifenberger, *Appl. Phys. Lett,.* **92**, 213112, 3pp, 2008.

[31] L. Dong, S. Youkey, J. Bush, J. Jiao, V. M. Dubin, R. V. Chebiam, *J. Appl. Phys.*, **101**, 024320, 7pp, 2007.

[32] A. Botman, J. J. L. Mulders, C. W. Hagen, *Nanotechnology* **20**, 372001,17pp, 2009.

[33] P. Wilhite, A. Vyas, Jason Tan, Jasper Tan, T. Yamada, P. Wang, J. Park, C. Y. Yang, *Semicond. Sci. Technol.*, 29, 054006, 16pp, 2014.